

RESEARCH ARTICLE

Editor's Choice

Mechanochemical Activation of a Metal–Organic Framework Embedded within a Thermoplastic Polyurethane Matrix: Probing Fluorogenic Stress-Sensing

*Kshitij Sanjay Shinde, Philipp Michael, and Wolfgang H. Binder**

Here, a mechanochemically triggered Cu(I) bis(*N*-heterocyclic carbene [NHC])-based metal–organic framework (MOF) embedded into a thermoplastic polyurethane (TPU)-matrix is reported. The induced fluorogenic copper-catalyzed azide–alkyne cycloaddition (CuAAC) reveals the stressed parts within the thermoplastic PU via a simple optical detection. As determined via oscillating tensile rheology on dumbbell-shaped samples of TPU, a MOF, containing 4.66% copper, catalyzes the fluorogenic CuAAC between the nonfluorescent precursor dyes, 8-azidonaphthalen-2-ol, and 3-hydroxyphenylacetylene. After mechanical activation of the MOF situated inside the TPU, the fluorescent 8-(4-(3-hydroxyphenyl)-1,2,3-triazol-1-yl)naphthalen-2-ol dye is formed. Monitoring the formation of the dye inside the TPU via fluorescence spectrometry at $\lambda_{\text{ex}} = 458 \text{ nm}$ shows an increase of the fluorescence intensity up to 60–70%. It is demonstrated that a dumbbell-shaped TPU, subjected to higher stress, displays higher fluorescence than the surrounding other areas, thus effectively functioning as a three-in-one stress-sensor system.

a decrease in the molecular weight of polymers during mechanical stress.^[2,3] From there on, functional groups termed mechanophores, specific chemical groups prone to activation by force,^[4–6] have been discovered and designed, which can be activated by various mechanical stimuli such as ultrasound^[7–12] and milling/liquid-assisted grinding (LAG).^[13–16]


When linear polymer chains or whole polymer networks are attached via covalent bonds to such mechanophores, they primarily facilitate transmittance of the force onto the central chemical bond depending on the position^[17,18] of the “mechanophore” within the polymer-chain, as longer chains facilitate bond breaking. This is not only proven experimentally, but also supported by theoretical methods such as constrained geometry to simulate forces (COGEF)-calculations.^[19,20] An increased polymer rigidity (higher glass-transition temperature^[21,22]) and increased chain length^[23] (longer polymer chains lead to enhanced bond rupture, stiffer chains via the higher T_g of polystyrene vs polyisobutylene) can promote mechanical activation more efficiently to the specific mechanophore.^[22] But, also the material morphology will influence activation, such as the location of the mechanophore within/between semicrystalline interphases,^[24,25] or at the interface in microphase segregated block copolymers.^[26,27] It is known that the flexibility of networks^[28] and their crosslinking density^[29,30] decide on the efficiency of mechanophoric activation. When several mechanophores are present in multiple amounts along a polymer main chain, bond-rupture is facilitated.^[31] Thus, mechanochemistry within a polymeric material has developed as an important chemical tool for applications such as stress-sensing/damage reporting^[32–36] to estimate a material's lifetime.^[37] Mechanophores such as 1,2-dioxetanes,^[38–43] spiropyrans,^[44–48] or rotaxanes,^[49–51] provide force-induced optical signals, often however only as a temporary response.^[29]

We in the past have developed a Cu(I) bis(*N*-heterocyclic carbene) (NHC) mechanophoric system,^[37] which can be embedded within polymer- and peptide backbones^[21,29,52–54] Such Cu(I) bis(NHC) complexes are capable of activation by mechanical forces transmitted via covalently attached polymer chains, coupled by a mechano-fluorescent approach. The applied external mechanical force thus resulted in the cleavage of one of

1. Introduction

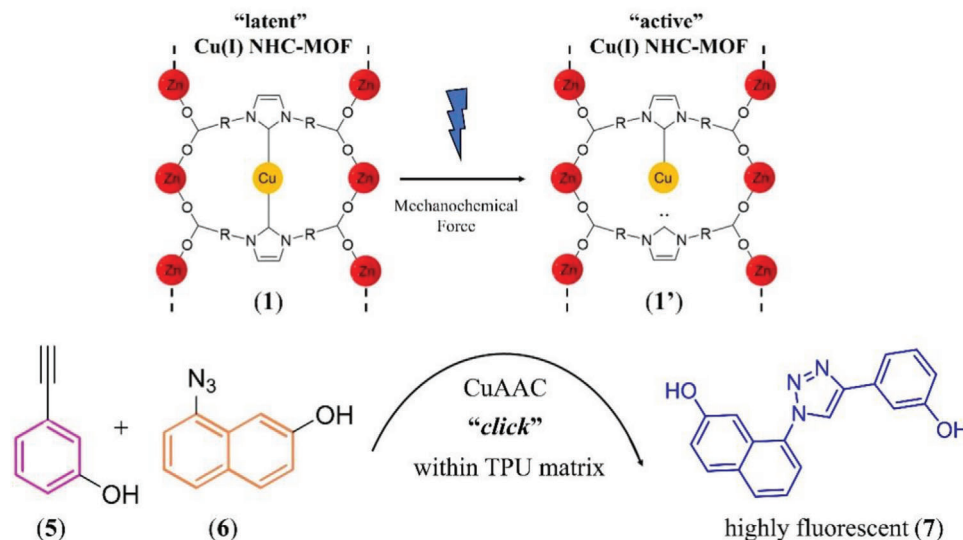
Chemical reactions driven by mechanical force or pressure instead of traditional activation such as thermal stimuli are known as mechanically induced reactions.^[1] Historically, this type of chemistry was observed in solid state-reactions, where covalent bonds are mechanically broken directly by an external force, noticed as early as in the 1930's when Staudinger observed

K. S. Shinde, P. Michael, W. H. Binder
 Macromolecular Chemistry
 Division of Technical and Macromolecular Chemistry
 Institute of Chemistry
 Faculty of Natural Science II (Chemistry, Physics and Mathematics)
 Martin Luther University Halle-Wittenberg
 Von-Danckelmann-Platz 4, D-06120 Halle (Saale), Germany
 E-mail: wolfgang.binder@chemie.uni-halle.de

 The ORCID identification number(s) for the author(s) of this article can be found under <https://doi.org/10.1002/macp.202300297>

© 2023 The Authors. Macromolecular Chemistry and Physics published by Wiley-VCH GmbH. This is an open access article under the terms of the Creative Commons Attribution-NonCommercial License, which permits use, distribution and reproduction in any medium, provided the original work is properly cited and is not used for commercial purposes.

DOI: 10.1002/macp.202300297



Scheme 1. Concept of a stress induced CuAAC “click” reaction between the nonfluorescent components (5) and (6) after mechanical activation of the embedded MOF (1) to form the activated MOF (1') inside a TPU network.

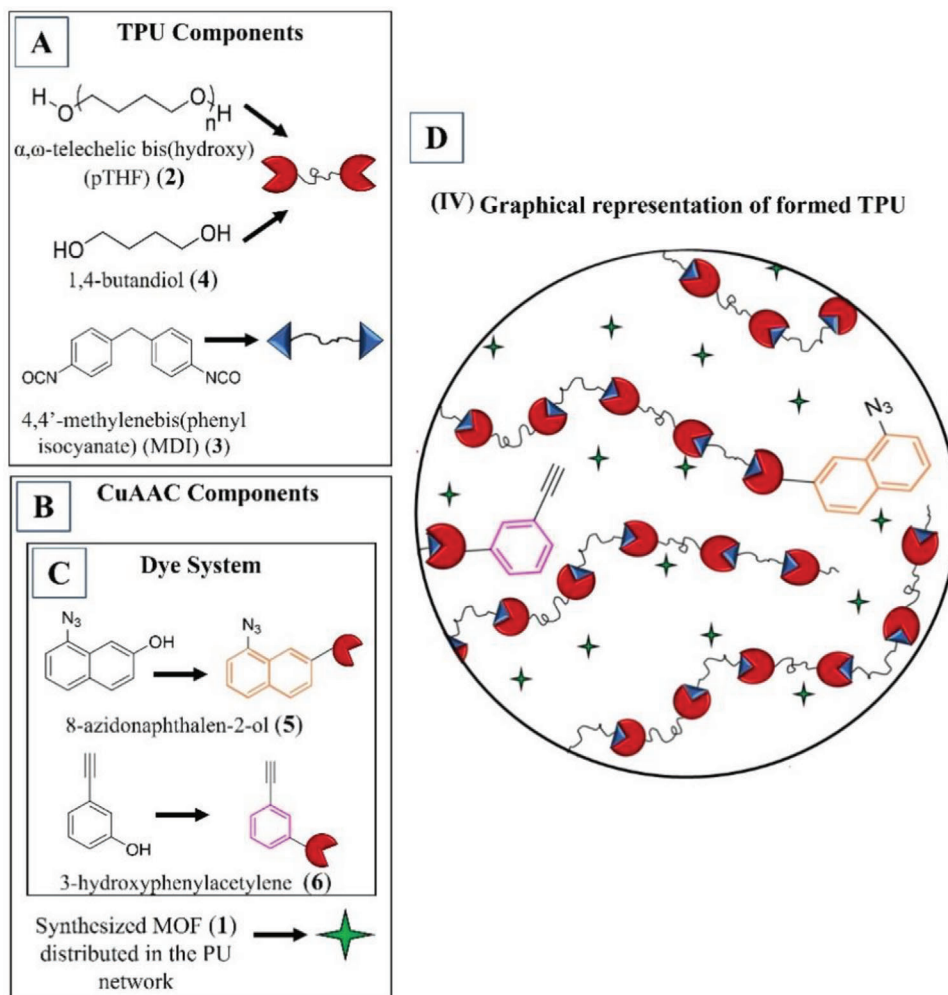
the two shielding NHC ligands attached to the initially inactive Cu(I) center, rupturing the mechanochemically labile bond present between the NHC-carbon and the Cu(I). We previously have reported the use of a metal–organic framework (MOF) containing the mechanophoric Cu(bis-NHC)-complex, proving its ultrasound-mediated mechanochemical activation via a fluorogenic copper-catalyzed “click”-reaction (CuAAC)-reaction of benzylazide and phenylacetylene to yield 1-benzyl-4-phenyl-1H-1,2,3-triazole.^[55] The coordination of the terminal alkyne with the now available Cu(I) of an active Cu(I) mono(NHC) forms the copper acetylide to subsequently promote the formation of the 1,2,3-triazole product,^[53,55] which can be easily quantified in a fluorogenic “click” reaction (see **Scheme 1**).

In an expansion of our previous work, we here report the successful integration of the MOF-mechanophore (1) into a polymeric (bulk) matrix consisting of a segmented polyurethane (thermoplastic polyurethane, TPU), composed of α,ω -telechelic bis(hydroxy) poly(tetrahydrofuran) (pTHF, (2)), 4,4'-methylenebis(phenyl isocyanate) (MDI, (3)) and the chain extender 1,4-butanediol (BDO, (4)). The primary objective of the study is to probe the mechanochemical activation of the MOF within a shape memory-TPU (SMPU) matrix of a defined stiffness. Furthermore, the mechanochemically activated MOF (1') can act as a trigger for a fluorogenic CuAAC of the covalently linked compounds 8-azidonaphthalen-2-ol (5) and 3-hydroxyphenylacetylene (6), forming the fluorescent 8-(4-(3-hydroxyphenyl)-1,2,3-triazol-1-yl)naphthalen-2-ol (7), via a fluorogenic “click”-reaction after stress has been imparted on the TPU (see **Scheme 1**). The concept is to develop strategies to obtain a three-in-one stress-sensor system that would: 1) undergo mechanochemical activation in the presence of an embedded Cu(I) bis(NHC)-containing MOF, 2) function inside a shape memory TPU material (SMPU), and 3) allows to monitor the mechanochemical activation process via a fluorogenic dye system.

2. Results and Discussion

We aimed to generate TPUs with a defined stiffness and strength, to further allow the embedding of the mechanochemically active MOF therein. The design of the synthesized TPU is shown in **Scheme 2** (more details are shown in **Scheme S1**, Supporting Information). Polyaddition reaction between pTHF (2) (poly(tetrahydrofuran) with $M_n = 2900 \text{ g mol}^{-1}$) and methylene-diisocyanate, MDI (3), in the presence of catalytic amounts of 1,8-diazabicyclo[5.4.0]undec-7-ene (DBU), generates pre-condensed soft block segments (**Scheme S1-I**, Supporting Information). Subsequent addition of the chain extender 1,4-butanediol, BDO (4), results in the formation of hard block segments, leading to the formation of alternating soft/hard blocks (see **Scheme S1-III**, Supporting Information)-based supramolecular crosslinked network via π – π bonding and strong hydrogen bonding among the urethane linkages.^[56] The chosen ratio of the soft/hard blocks influences the physical properties of the TPU. An increasing percentage of hard blocks leads to an increased tensile strength and Young's modulus, thus resulting in an increasing rigidity.^[57,58] In our initial experiments with varying soft/hard block ratios (see **Table S1**, Supporting Information), we noticed that TPUs composed of a low hard segment ratio (30%, TPU30) ruptured almost immediately under force, while the high hard segment ratio TPUs (70%, TPU70) could not be measured accurately with oscillating tensile rheology due to its rigidity. Therefore, a soft/hard ratio of 50:50 (TPU50) was chosen for the embedding of the components necessary for CuAAC (see **Scheme 2B**), which includes the dye system and the mechanochemically active MOF (1) (see **Scheme 2**).

Subsequently, the fluorogenic dye precursors (5 and 6) and the mechanochemically active MOF (1) were embedded into a TPU50-composition as depicted in **Scheme 2**. The 8-azidonaphthalen-2-ol (5) (see Supporting Information for synthesis and characterization) and 3-hydroxyphenylacetylene (6) were



Scheme 2. Schematic concept for the synthesis of a stress-sensing thermoplastic polyurethane (TPU) consisting of (A, B, C) the TPU components and components necessary to conduct copper-catalyzed click chemistry (CuAAC), (5) and (6) and the MOF (1). D) Schematic representation of the formed TPU including all components.

embedded covalently into the TPU network in concentrations of $10 \mu\text{mol g}^{-1}$ of TPU (with a total weight including all components (2), (3), and (4) of $\approx 7.23 \text{ g}$) via the $-\text{OH}$. As the MOF (1) (6 mg of (1), with 4.66 wt.% Cu (0.06 eq of Cu:1 eq. of (5)/(6))) is insoluble in most solvents, it was dispersed so as to distribute it into the formed TPU (for detailed synthesis procedure, see SI). Gel permeation chromatography (GPC) analysis of the native TPU50 without (1) yielded a molecular weight M_n of $\approx 65 \text{ kDa}$, with a polydispersity index (PDI) of 1.95 (retention volume = 6.2 mL). The final obtained TPU system is conveyed as a graphical representation in Scheme 2(IV).

Various TPU50 samples were prepared for different purposes. A set of reference TPU50 samples, embedded with varying concentrations of (5), (6), and (7) (Table 1, Entry 4–Entry 7), were prepared to mimic different percentages of conversion of (5) and (6) to (7), as part of a series of measurements referred to as fluorescence test measurements (FTM, see Section 4.2.1), Supporting Information. Based on previously conducted optical measurements of the click dye (7) (UV-vis and fluorescence measure-

ments in solution),^[29] an excitation wavelength (λ_{ex}) of 377 nm was chosen.

The mode of embedding the MOF (1) into the TPU proved important: the first attempts used mechanical stirring, TPU50_Stir (Table 1, Entry 1), to disperse the MOF before introducing it within TPU50, resulting in an already primordial fluorescence (see Figure 1A) at $\lambda_{\text{em}} = 458 \text{ nm}$ (at $\lambda_{\text{ex}} = 377 \text{ nm}$). This is attributed to the methodology of suspending the MOF (1) by stirring (see Table S2, Supporting Information), resulting in the formation of an already activated MOF (1') (see Scheme 3), with a visible CuAAC in the TPU solution before solidification.^[55] We therefore chose another strategy for dispersion by dispersing the MOF via ultrasonication in an ultrasonication bath for times of either 10 mins (TPU50_USB1 (Table 1, Entry 2)) or 10 s (TPU50_USB2 (Table 1, Entry 3)). Shorter ultrasonication times (10 s) resulted in only a low level of this primordial activation (see Figure 1A) in the sample TPU50_USB2 (Table 1, Entry 3). This methodology proved to be effective as the initial fluorescence in TPU50_USB2 showed a 72% decrease over TPU50_Stir (29 a.u.

Table 1. Composition of the TPU50-samples according to detailed procedures described in the SI.

Entry No.	Application Code	MOF (1)	TPU Components			Precursor Dyes		(7) Moles [μ mol]
			(2)	(3)	(4)	(5)	(6)	
			Mass [mg]	Moles [mmol]	Moles [mmol]	Moles [mmol]	Moles [μ mol]	
Stretching Experiment Samples								
1	TPU50_Stir ^{a, b)}	6.0	2.1	4.1	2.1	72.3	72.3	–
2	TPU50_USB1 ^{a, b)}	6.0	2.1	4.1	2.1	72.3	72.3	–
3	TPU50_USB2 ^{a)}	6.0	2.1	4.1	2.1	72.3	72.3	–
Reference TPU50 for Fluorescence Test Measurements (FTM)								
4	FTM.0%	–	2.1	4.1	2.1	72.3	72.3	0.0
5	FTM.25%	–	2.1	4.1	2.1	54.0	54.0	18.0
6	FTM.50%	–	2.1	4.1	2.1	36.2	36.2	36.2
7	FTM.75%	–	2.1	4.1	2.1	18.0	18.0	54.0

^{a)} Refer to Table S2 (Supporting Information) for detailed description of the samples of entries 1, 2, and 3; ^{b)} These samples were additionally used to probe the shape memory of TPU (SMPU).

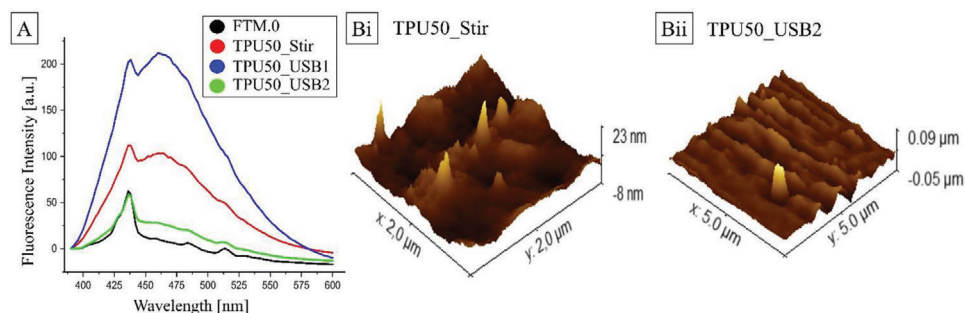
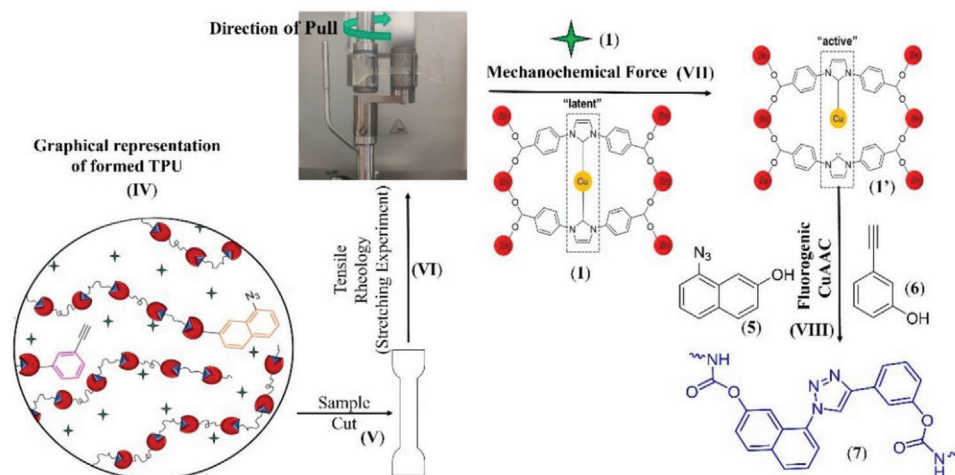


Figure 1. Fluorescence spectroscopy on TPUS using different methods of preparing TPU50 samples : A) the fluorescence intensities before stretching experiments are conducted due to primordial activation, and B) the differences in MOF sizes embedded within the TPU seen in the 3D AFM images obtained of i) TPU50_Stir and ii) TPU50_USB2.



Scheme 3. Schematic concept for the mechanochemical activation of a latent MOF (1) within a solid thermoplastic polyurethane (TPU) to catalyze a subsequent fluorogenic copper-catalyzed click chemistry (CuAAC) to form the highly fluorescent 8-(4-(3-hydroxyphenyl)-1,2,3-triazol-1-yl)naphthalen-2-ol dye (7).

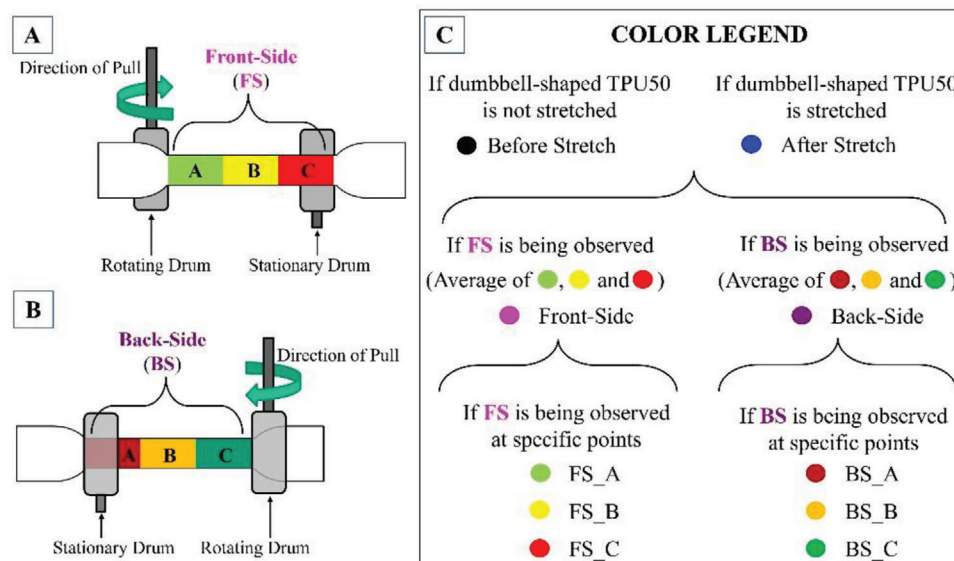


Figure 2. Schematic depiction of the stretching regions to describe the areas on which fluorescence spectrometry was conducted in a dumbbell-shaped TPU50 sample.

in TPU50_USB2), comparable now to the fluorescence spectrum displayed by a sample devoid of the fluorescent dye (7), but containing the initial dye-components, FTM.0% (Table 1, Entry 4). The size of the MOF (1) particles in the samples TPU50_Stir (14 nm) and TPU50_USB2 (85 nm), as observed in the AFM measurements (see Figure 1B), was attributed to the different dispersion methods, clearly indicating that TPU50_USB2 with its larger MOF (1) particles exhibited a lower initial catalytic behavior.^[55]

The TPU50 embedded with MOF (1), (5), and (6) was then subjected to oscillating tensile rheology, for which the samples were cut to obtain dumbbell-shaped samples using a sample cutter (see Scheme 3(V)). Oscillating tensile rheology was conducted via a “Universal Extensional Fixture (UXF)” by repeatedly applying

stress over multiple cycles. A single cycle was designed such that, as depicted in Scheme S4 (Supporting Information), stretching (stressing/damaging) was conducted for 60 mins at 25 °C with a deformation of 40% and a frequency of 0.5 Hz. This was followed by 30 mins of heating at 50 °C directly inside the oven of the UXF to recover material properties by melting the soft block of the TPU, triggering shape-memory behavior. Subsequently, a waiting period of further 75 mins at 25 °C was observed to recover the properties of the TPU (Scheme S4, Supporting Information). Based on previous control experiments conducted for MOF (1) in solution only a limited thermal activation at 60 °C had occurred for a duration of 50 h.^[55] We thus can exclude that MOF (1) plays a significant role in promoting a CuAAC at a temperature of 50 °C

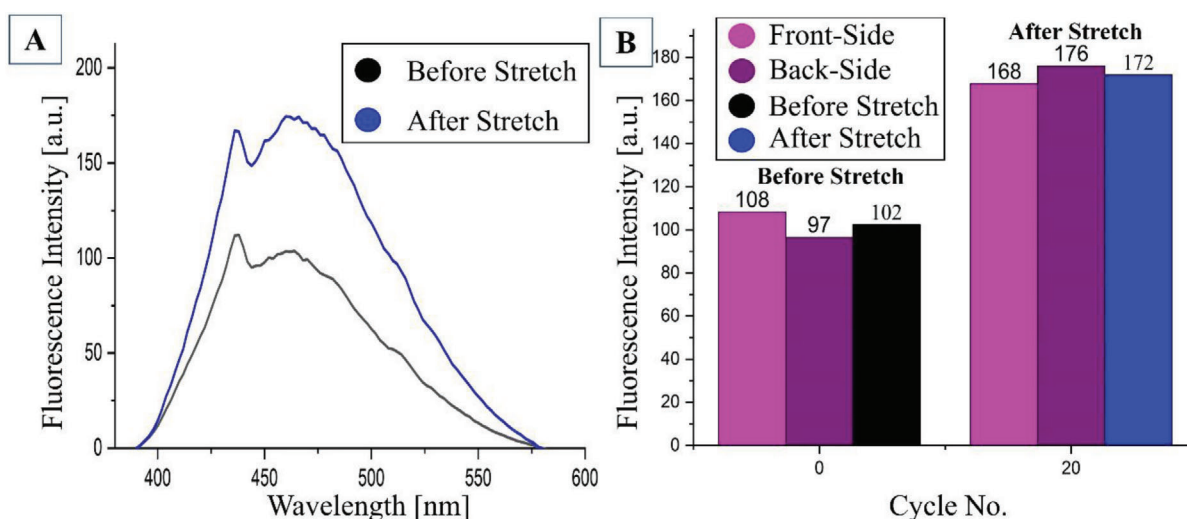


Figure 3. Oscillating tensile rheology resulted in quantifiable fluorescence intensities, achieved with $\lambda_{ex} = 377$ nm and displayed in the form of a A) fluorescence spectrum before and after the stretching experiment, as well as a B) graph displaying the intensities at $\lambda_{ex} = 458$ nm. The colors of both (A) and (B) correspond to the colors indicated in stretching terms indicated in Figure 2.

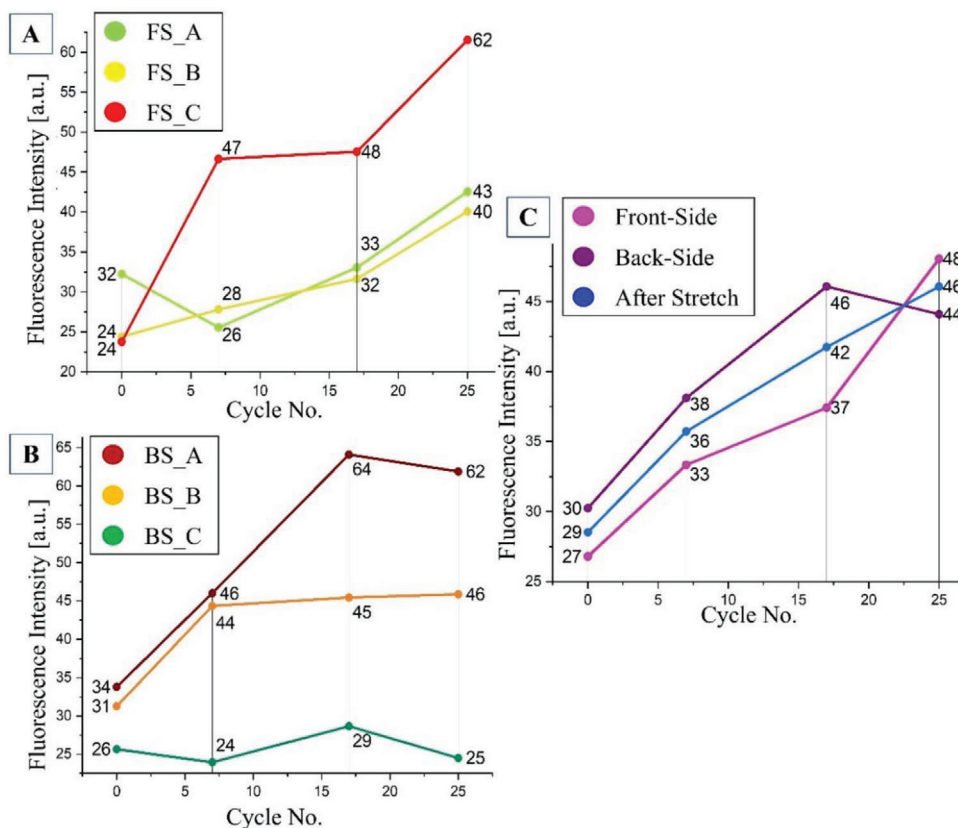


Figure 4. The stretching experiments of TPU50_USB2 resulted in fluorescence at $\lambda_{\text{ex}} = 377$ nm. Intensities achieved at $\lambda_{\text{em}} = 458$ nm over 25 cycles indicate an increasing fluorescence attributed to (7) observed in A) Front-Side, B) Back-Side, and C) an average of the two Sides. The colors of (A), (B), and (C) correspond to the colors indicated in stretching terms in **Figure 2**.

over 12.5 h (30 mins per cycle, 25 cycles) in bulk, thus justifying the chosen parameters for the measurements.

Further the shape memory properties of the TPU (SMPU) containing MOF (1) were probed via a brief study of the thermally induced shape memory effect. SMPU is not an inherent property of any PU but that of a segmented PU, i.e., TPU, and is triggered by different external stimuli.^[59] The segmentation, caused by microphase separation, is due to incompatibility between phases, leading to the formation of soft and hard block segments.^[60,61] The shape memory efficiency and the recovery efficiency were evaluated over 20 cycles (see Figure S9, Supporting Information) using Equations S1 and S2 (Supporting Information). Two different samples of TPU50, namely TPU50_Stir and TPU50_USB1 (see Table 1, **Entry 1** and **2**) were used, each embedded with the precursor dyes (5) and (6), and the MOF (1). The independently conducted experiments provided two sets of data which were averaged to enhance accuracy. Over 20 cycles, the shape memory efficiency remained in the 90–96% range while the recovery efficiency remained in the 80–100% range (see Table S3, Supporting Information), thus excluding the possibility that the mechanochemical activation might be induced by any changes of the physical properties of the TPU.

We then tested the mechanochemical activation of MOF (1) within a TPU-fluorogenic dye system (**Figure 2**). Additionally, fluorescence test measurements (FTM) were conducted with the synthesized TPU50 as a control experiment with varying concen-

trations of the precursor dyes (5 and 6) and the click dye (7) (see Table 1, **Entry 4–Entry 7**), without embedding the MOF (1) as the mechanocatalyst inside the TPU50 (see Supporting Information for more details) to observe the subsequent fluorescence emission spectra. Varying the concentrations of the click dye (7) in the TPU50 via the increasing fluorescence at $\lambda_{\text{em}} = 458$ nm of (7), a calibration curve could be generated (Figure S10, Supporting Information) to subsequently quantify the extent of the click-reaction after stretching.

We then probed the activation of samples prepared by different methodologies. For the stretching experiments, TPU50_Stir and TPU50_USB2 samples (Table 1, **Entry 1** and **Entry 3**), both embedded with MOF (1), (5), and (6), were investigated. The first stretching experiment was conducted on the dumbbell-shaped TPU50_Stir sample (Table 1, **Entry 1**). Based on the measurements of the samples on both sides (Front-Side (FS) and Back-Side (BS)) at different positions (positions A, B, and C) as presented in Figure 2, after 20 cycles of stretching, the fluorescence intensity showed an overall increase of 69% ($102 \rightarrow 172$ a.u.) (see **Figure 3B**).

Furthermore, the position FS_C shows a much higher intensity than FS_A while BS_A shows a much higher intensity than BS_C (see Figure S11, Supporting Information). These variations in intensities are remarkable if compared to the intensities before stretching as then the intensities were quite similar and formed an excellent comparable starting point, marking the

conceptual idea as successful. The detailed % increase at specific points of the TPU50_Stir sample is presented in Table S5 (Supporting Information). After the success of the first measurement, a more detailed stretching experiment was conducted with TPU50_USB2 (see Table 1, **Entry 3**). After 25 cycles of stretching, the fluorescence intensity showed an increase of 59% (29 → 46 a.u., see **Figure 4**). Hence, the effect of increase in fluorescence by an external application of stress to activate the latent MOF (1) was achieved in both samples, TPU50_Stir and TPU50_USB2.

We noted that there is a significant difference in activation depending on certain parts of the samples (see **Figure 2**) whether the Front- (FS) or the Back-Side (BS) of the samples were measured. **Figure 4** (sample TPU50_USB2) shows that in the case of the Front-Side, FS_A, and FS_C show an increase of 34% and 158% respectively, while in the case of the Back-Side, BS_C shows almost no increase while BS_A shows an increase of 82% (see Table S6, Supporting Information). After conducting several series of experiments, we found this to be well reproducible, with the effect being more pronounced to the positions A, B, and C along the stretching axis, rather than the front/backside effect. Overall, the different experiments together show the effect of stretching on the mechanophoric MOF (1) embedded TPU, demonstrating that they can be used as a fluorogenic stress-sensor. Additionally, the areas of the TPU receiving higher stress showed higher fluorescence, assisting in pin-pointing specific areas within the TPU with an increased possibility of material failure.

3. Conclusion

In conclusion, we have achieved a three-in-one stress-sensor system inside a shape memory thermoplastic polyurethane (TPU) as the solid matrix, embedding a mechanophore to achieve a stretching-induced, mechanochemically triggered CuAAC, resulting in a monitorable fluorogenic dye. A functional mechanophoric Cu(I) bis(NHC) based metal-organic framework MOF (1) was embedded within a multicomponent TPU along with a recently developed fluorogenic dye based on covalently bound 8-azidonaphthalen-2-ol (5) and 3-hydroxyphenylacetylene (6), resulting in quantification of the exerted stress inside the material via the fluorescent 8-(4-(3-hydroxyphenyl)-1,2,3-triazol-1-yl)naphthalen-2-ol dye (7) on basis of a CuAAC. There is a correlation between the applied stress and the observed fluorescence, depending on the position of the measurements. We presume that this approach holds a viable approach toward stress-sensing parts in widely used PU-networks, which can easily be applied to a multitude of different material via easily applicable polyurethanes.

Supporting Information

Supporting Information is available from the Wiley Online Library or from the author.

Acknowledgements

This research was funded by the European Social Funds (ESF) and the State of Saxony-Anhalt through the graduate school AGRIPOLY and the

GRK 2670 (TP B2) as well as the Deutsche Forschungsgemeinschaft (DFG) - Projektnummer 506699569 (Spannung und Ciralitätstransfer). The authors would like to thank Dr. Daniel Fuhrmann for measuring and assisting in the characterization of the MOF by PXRD and Dr. Anja Marinow for her diligent guidance throughout the progress of this work.

Open access funding enabled and organized by Projekt DEAL.

Conflict of Interest

The authors declare no conflict of interest.

Data Availability Statement

The data that support the findings of this study are available in the supplementary material of this article.

Keywords

CuAAC, fluorogenic stress-sensor, mechanochemical activation, metal-organic frameworks, N-heterocyclic carbenes

Received: August 14, 2023

Revised: September 20, 2023

Published online: October 19, 2023

- [1] N. R. Sottos, *Nat. Chem.* **2014**, *6*, 381.
- [2] H. Staudinger, W. Heuer, *Ber. Dtsch. Chem. Ges.* **1934**, *67*, 1159.
- [3] G. Kaupp, *CrystEngComm* **2009**, *11*, 388.
- [4] D. A. Davis, A. Hamilton, J. Yang, L. D. Cremar, D. Van Gough, S. L. Potisek, M. T. Ong, P. V. Braun, T. J. Martinez, S. R. White, J. S. Moore, N. R. Sottos, *Nature* **2009**, *459*, 68.
- [5] A. Piermattei, S. Karthikeyan, R. P. Sijbesma, *Nat. Chem.* **2009**, *1*, 133.
- [6] J. F. S. Yu, J. L. Zakin, G. K. Patterson, *J. Appl. Polym. Sci.* **1979**, *23*, 2493.
- [7] K. S. Suslick, G. J. Price, *Annu. Rev. Mater. Sci.* **1999**, *29*, 295.
- [8] J. M. J. Paulusse, J. P. J. Huijbers, R. P. Sijbesma, *Chemistry* **2006**, *12*, 4928.
- [9] G. Cravotto, E. C. Gaudino, P. Cintas, *Chem. Soc. Rev.* **2013**, *42*, 7521.
- [10] H. N. a. Kim, K. S. Suslick, *Chemistry* **2017**, *23*, 2778.
- [11] R. Küng, R. Göstl, B. M. Schmidt, *Chemistry* **2022**, *28*, e202103860.
- [12] L. i. Tu, Z. Liao, Z. Luo, Y.-L. Wu, A. Herrmann, S. Huo, *Exploration* **2021**, *1*, 20210023.
- [13] J.-L. Do, C. Mottillo, D. Tan, V. Strukil, T. Friscic, *J. Am. Chem. Soc.* **2015**, *137*, 2476.
- [14] R. Thorwirth, A. Stolle, B. Ondruschka, A. Wild, U. S. Schubert, *Chem. Commun.* **2011**, *47*, 4370.
- [15] H. He, G. Di, X. Gao, X. Fei, *Chemosphere* **2020**, *243*, 125339.
- [16] D. V. Kravchuk, T. Z. Forbes, *Chem. Commun.* **2022**, *58*, 4528.
- [17] K. L. Berkowski, S. L. Potisek, C. R. Hickenboth, J. S. Moore, *Macromolecules* **2005**, *38*, 8975.
- [18] S. Neumann, M. Biewend, S. Rana, W. H. Binder, *Macromol. Rapid Commun.* **2020**, *41*, 1900359.
- [19] M. K. Beyer, H. Clausen-Schaumann, *Chem. Rev.* **2005**, *105*, 2921.
- [20] I. M. Klein, C. C. Husic, D. P. Kovács, N. J. Choquette, M. J. Robb, *J. Am. Chem. Soc.* **2020**, *142*, 16364.
- [21] P. Michael, S. K. Sheidaee Mehr, W. H. Binder, *J. Polym. Sci. Pol. Chem.* **2017**, *55*, 3893.
- [22] P. Michael, W. H. Binder, *Angew. Chem., Int. Ed.* **2015**, *54*, 13918.
- [23] M. J. Kryger, A. M. Munaretto, J. S. Moore, *J. Am. Chem. Soc.* **2011**, *133*, 18992.

- [24] C. K. Lee, B. A. Beiermann, M. N. Silberstein, J. Wang, J. S. Moore, N. R. Sottos, P. V. Braun, *Macromolecules* **2013**, *46*, 3746.
- [25] S. He, M. Stratigaki, S. P. Centeno, A. Dreuw, R. Göstl, *Chemistry* **2021**, *27*, 15889.
- [26] A. L. Black Ramirez, J. W. Ogle, A. L. Schmitt, J. M. Lenhardt, M. P. Cashion, M. K. Mahanthappa, S. L. Craig, *ACS Macro Lett.* **2012**, *1*, 23.
- [27] Z. Huo, S. Arora, V. A. Kong, B. J. Myrnga, A. Statt, J. E. Laaser, *Macromolecules* **2023**, *56*, 1845.
- [28] T. A. Kim, M. J. Robb, J. S. Moore, S. R. White, N. R. Sottos, *Macromolecules* **2018**, *51*, 9177.
- [29] M. Biewend, P. Michael, W. H. Binder, *Soft Matter* **2020**, *16*, 1137.
- [30] E. M. Lloyd, J. R. Vakil, Y. Yao, N. R. Sottos, S. L. Craig, *J. Am. Chem. Soc.* **2023**, *145*, 751.
- [31] M. Biewend, S. Neumann, P. Michael, W. H. Binder, *Polym. Chem.* **2019**, *10*, 1078.
- [32] D. W. R. Balkenende, S. Coulibaly, S. Balog, Y. C. Simon, G. L. Fiore, C. Weder, *J. Am. Chem. Soc.* **2014**, *136*, 10493.
- [33] R. Göstl, R. P. Sijbesma, *Chem. Sci.* **2016**, *7*, 370.
- [34] N. Willis-Fox, E. Watchorn-Rokutan, E. Rognin, R. Daly, *Trends Chem.* **2023**, *5*, 415.
- [35] M. Stratigaki, R. Göstl, *ChemPlusChem* **2020**, *85*, 1095.
- [36] M. E. Mcfadden, M. J. Robb, *J. Am. Chem. Soc.* **2021**, *143*, 7925.
- [37] M. Philipp, W. H. Binder, *Angew. Chem., Int. Ed.* **2015**, *54*, 13918.
- [38] Y. Chen, A. J. H. Spiering, S. Karthikeyan, G. W. M. Peters, E. W. Meijer, R. P. Sijbesma, *Nat. Chem.* **2012**, *4*, 559.
- [39] J. M. Clough, A. Balan, T. L. J. Van Daal, R. P. Sijbesma, *Angew. Chem., Int. Ed.* **2016**, *55*, 1445.
- [40] E. Ducrot, Y. Chen, M. Bulters, R. P. Sijbesma, C. Creton, *Science* **2014**, *344*, 186.
- [41] T. Hirano, C. Matsuhashi, *J. Photoch. Photobio. C* **2022**, *51*, 100483.
- [42] Y. Shen, Y. Yuan, X. Ma, W. Yang, Y. Chen, *Polym. Chem.* **2023**, *14*, 4148.
- [43] J.-H. Zhang, S. Liu, Y. Yuan, Y.-L. Chen, *Chinese J. Polym. Sci.* **2023**, *41*, 1162.
- [44] C. M. Kingsbury, P. A. May, D. A. Davis, S. R. White, J. S. Moore, N. R. Sottos, *J. Mater. Chem.* **2011**, *21*, 8381.
- [45] B. A. Beiermann, S. L. B. Kramer, J. S. Moore, S. R. White, N. R. Sottos, *ACS Macro Lett.* **2012**, *1*, 163.
- [46] S. L. Potisek, D. A. Davis, N. R. Sottos, S. R. White, J. S. Moore, *J. Am. Chem. Soc.* **2007**, *129*, 13808.
- [47] Z. Cao, *Macromol. Chem. Phys.* **2020**, *221*, 2000190.
- [48] R. Janissen, G. A. Filonenko, *J. Am. Chem. Soc.* **2022**, *144*, 23198.
- [49] Y. Sagara, M. Karman, E. Verde-Sesto, K. Matsuo, Y. Kim, N. Tamaoki, C. Weder, *J. Am. Chem. Soc.* **2018**, *140*, 1584.
- [50] J. Yang, Y. Xia, *CCS Chem.* **2023**, *5*, 1365.
- [51] T. Muramatsu, Y. Okado, H. Traeger, S. Schrettl, N. Tamaoki, C. Weder, Y. Sagara, *J. Am. Chem. Soc.* **2021**, *143*, 9884.
- [52] P. Michael, M. Biewend, W. H. Binder, *Macromol. Rapid Comm.* **2018**, *39*, 1800376.
- [53] S. Funtan, P. Michael, W. H. Binder, *Biomimetics* **2019**, *4*, 24.
- [54] S. Funtan, A. Funtan, R. Paschke, W. Binder, *Org. Mater.* **2020**, *02*, 116.
- [55] K. S. Shinde, P. Michael, D. Fuhrmann, W. H. Binder, *Macromol. Chem. Phys.* **2023**, *224*, 2200207.
- [56] K. Imato, T. Kanehara, S. Nojima, T. Ohishi, Y. Higaki, A. Takahara, H. Otsuka, *Chem. Commun.* **2016**, *52*, 10482.
- [57] K. Nakamae, T. Nishino, S. Asaoka, Sudaryanto, *Int. J. Adhes. Adhes.* **1996**, *16*, 233.
- [58] A. Elidrissi, O. Krim, S. Ousslimane, *Pigm. Resin Technol.* **2008**, *37*, 73.
- [59] M. Behl, A. Lendlein, *Mater. Today* **2007**, *10*, 20.
- [60] S. Mondal, *Polym-Plast. Techn. Mat.* **2021**, *60*, 1491.
- [61] Y. Q. Fu, W. M. Huang, J. K. Luo, H. Lu, in *Shape Memory Polymers for Biomedical Applications*, (Ed.: L. H. Yahia), Woodhead Publishing, Cambridge, UK, **2015**, 167.